THERMAL VACUUM TESTING STRATEGY AND THERMAL DESKTOP MODEL CORRELATION FOR THE MOON TO MARS PLANETARY AUTONOMOUS CONSTRUCTION TECHNOLOGIES (MMPACT) ROBOTIC TERRESTRIAL ARM

Savanna Lyles
NASA Marshall Space Flight Center, Huntsville AL 35812

ABSTRACT

This paper discusses the initial thermal vacuum testing of the MMPACT robotic terrestrial arm. The robotic arm is part of a construction system designed for the lunar south pole surface. The first thermal vacuum test was a risk mitigation test to ensure the arm could operate in vacuum, with all other data collection as secondary priorities. 44 thermocouples (TCs) were attached to the arm. Installation was done with additional care to account for both the extra wiring harness weight on the arm with the TC wires and increased focus on stabilizing the TC attachments to the moving components. Thermal steady state of <= 0.01°C/hour was reached for the hot set of testing conditions. This data was used to correlate the Thermal Desktop (TD) model to the test results within +/- 5°C.

ACRONYMS

EE	End Effector
ESSCA	Engineering Services and Science Capability Augmentation Contract
ET	Environmental Test
ε	Infrared Emissivity
HCB	Heater Control Board
J0, J1…	Joint 0, Joint 1, etc.
LN2	Liquid Nitrogen
MGSE	Mechanical Ground Support Equipment
MMPACT	Moon To Mars Planetary Autonomous Construction Technologies
MSFC	Marshall Space Flight Center
RTD	Resistance Temperature Detector
TA	Terrestrial Arm
TC	Thermocouple
TD	Thermal Desktop
TVAC	Thermal Vacuum
V20	Thermal Vacuum Chamber #V-20
VMX	Vitreous Material Transformation

INTRODUCTION

The Moon to Mars Planetary Autonomous Construction Technologies (MMPACT) program is a research and technology development project at NASA with the goal of developing a construction system to use insitu resources on the Moon as building material. The Olympus project under the MMPACT program is to design a robotic arm system to process and manipulate lunar regolith. The end effector will include a high-power laser to heat the lunar regolith to melting temperatures for generating structures.

The robotic arm prototype system (called the “terrestrial arm”) was developed and component tested for vacuum by the vendor, ICON, to prepare for a full system test at MSFC. The terrestrial arm design also includes a counterweight to operate in Earth’s gravity. The most thermally sensitive components were the joints on the arm, due to the ball bearing lubrication requiring a relatively narrow temperature range as compared to the lunar environment. The arm design included electronic strip heaters applied to the outside of the joints to maintain the bearing temperature above its minimum operating limit of -10°C. The prototype did not include the end effector systems, instead having a mass simulator on the end of the arm. The terrestrial arm geometry with the mass simulator in place of the end effector is shown in Figure 1. There are three large joints, with arm beams in between those joints, and three small joints in series at the end of the arm, for six joints in total. To specify which joint is being discussed, they are numbered down the arm from 0 to 5. The initial joint, joint 0, is affixed to a pedestal with a thermal spacer made of G10 for test operations. The arm beams have cable trays (not shown in model) to contain the wiring for power to the arm, communications, and power to the heaters. When outstretched to its maximum length, the arm is roughly 15.5 feet long.

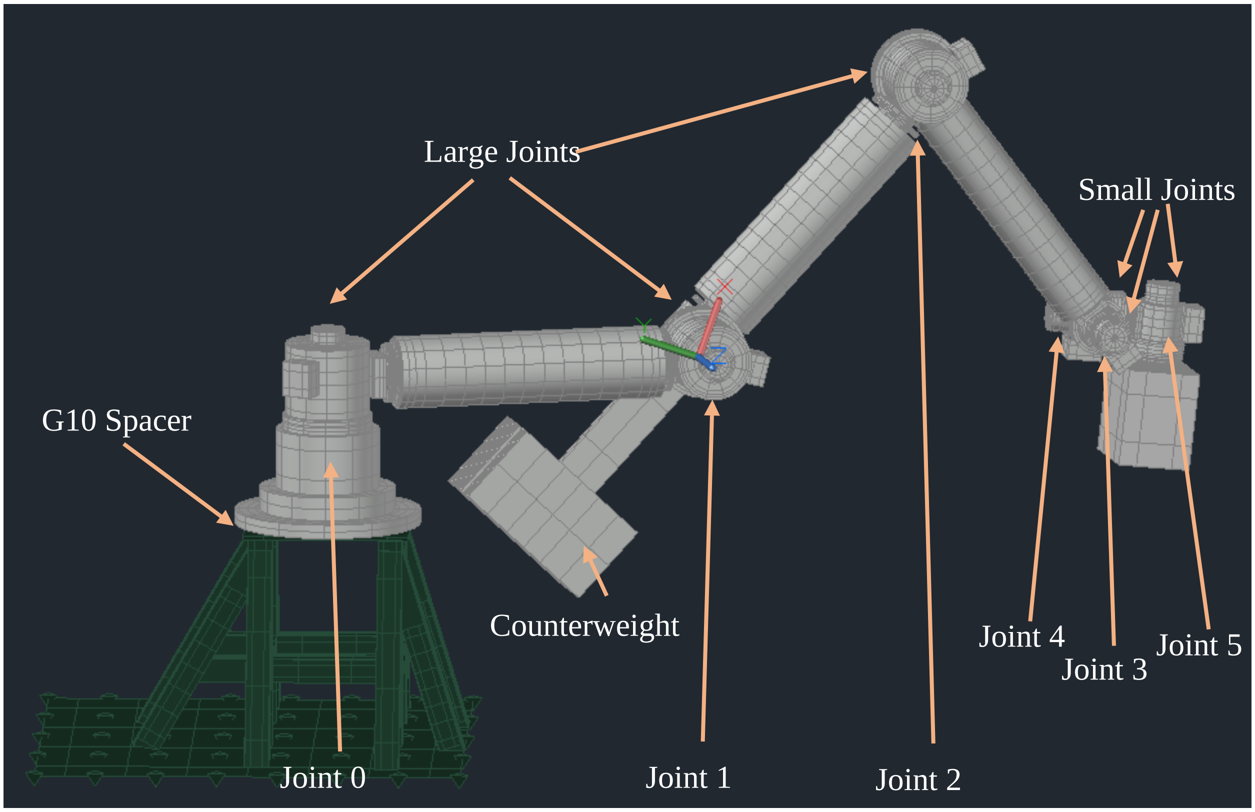

Figure 1. Terrestrial arm model shown in TD.

The initial testing aimed to verify the mechanical operation of the arm before moving on to test the arm with its end effector systems, to either confirm the physical design of the arm was sufficient to proceed or to gather data to refine the design. The preliminary thermal vacuum (TVAC) test for the Olympus arm was held in the Environmental Test Facilities (ET) V20 chamber due to the large size of the robotic arm. The initial testing aimed to verify the mechanical operation of the arm before testing the arm including its end effector systems, to either confirm the mechanical and software design of the arm was sufficient to proceed or to gather data to refine the design. None of the primary objectives required meeting pass/fail criteria as outlined in the ICON test documentation due to being defined as an engineering characterization and evaluation test. The primary and secondary test objectives defined in the MMPACT Terrestrial Arm (TA) Hardware Validation Test 1 Thermal Vacuum Procedure (ES61-TCP-MMPACT-001) are shown in Tables 1 and 2.

Table 1. Primary Test Objectives

Primary Objective	Objective Breakdown
Operational and logistical dress rehearsal of next test in both ambient and TVAC operations	Execute logistical tasks such as lifting/packing/shipping
	Execute robotic arm and V-20 chamber operations

	Implement multi-organizational roles and responsibilities
Verify the robotic arm system capability in TVAC	Confirm the system (comprised of electromechanical and software element system (comprised of electromechanical and software elements) will meet next test objectives
	Exercise the procedural framework necessary to produce laser vitreous material transformation (VMX)
Verify the TA's actuators' heater control boards (HCBs), heaters, and resistance temperature detectors (RTDs) in TVAC	Utilize the HCBs, heaters, and RTDs to self-heat the TA actuators to 57°C during hot TVAC testing
	Utilize the HCBs, heaters, and RTDs to maintain acceptable actuator temperatures during cold TVAC testing (liquid nitrogen [LN2]-flooded shroud) as defined procedurally
	Utilize the HCBs, heaters, and RTDs to warm the actuators to a temperature above the room dew point prior to breaking vacuum at the end of testing

Table 2. Secondary Test Objectives

Secondary Objective
Execute thermocouple and accelerometer data collection in support of thermal and structural/dynamic model development
Perform a modal test ("tap test") on the TA (with end effector [EE] simulator) in ambient conditions in one or more poses
Execute coordinated robotic arm motion similar to what will be necessary to support VMX production in Task 30
Execute off-arm TVAC checkouts of EE-related components and subsystems
Confirm functionality of laser cooling lines utilizing a "dead" laser inside of the chamber as well as coolant pump outside of the chamber
Demonstrate the ability of the TA to lift and move "MGSE blocks" that represent the approximate mass of a scoop of simulant or load needed to compress the simulant during VMX production

These primary objectives define three TVAC environments: no thermal control, a "hot" case using the arm heaters to raise the arm temperature to 57°C, and a "cold" case where the shroud is flooded with LN2 while the heaters maintain the arm at or above -10°C.

This was a sizeable constraint to the thermal analysis, as there was no guarantee of gathering steady state temperature data during this test. The test plan allowed for flexibility in what data was able to be gathered around the required operating motions but did not require a steady state thermal data to achieve a successful test. Test flexibility allowed the secondary objective of reaching steady state in the hot environment to be achieved. This is discussed in more detail in the test procedure section.

METHODS

Testing Overview

ICON designed a TVAC test procedure to perform a functional check of the arm movement at different thermal environments. The terrestrial arm was installed in the thermal vacuum chamber and pumped down to below 1e-5 Torr. The series of movements were performed without additional heating or cooling. The heater controls for the arm were then set to maintain 57°C on the joints. The series of movements were repeated for these hot conditions. The chamber shroud was then flooded with LN2, which creates a cold radiative environment with the shroud at an average temperature of -170°C while the heaters are set to maintain 0°. The series of movements were repeated for a final time in these cold conditions.

Test Configuration

The thermal vacuum chamber used was chamber V-20 at MSFC, which is part of the Environmental Test (ET) Facilities complex. This chamber was chosen due to its maximum test article area being 17’ by 22’ and therefore sufficient to contain the entire assembled arm. The chamber has a loading cart to allow for assembly or setup of test articles and can be then rolled inside the chamber. A pedestal for mounting the arm was designed and machined for the test. This was bolted onto the grate flooring of the cart and then the arm was bolted onto the pedestal. To thermally isolate the arm, a G10 spacer between the pedestal and the base of the arm was designed and machined. This was installed during the test article setup.

The chamber shroud is painted Catalac Black and is capable of being flooded with LN2 to cool the chamber. This allows for the shroud temperature to reach an average of -170°C.

Thermocouple Installation

Temperature sensor recommendations were made to measure each side of all mechanical and rotational joints, as well as points on the arm beams to gather data for model correlation. Since either side of each rotational joint also had mechanical bolted joints, 44 TCs were installed in total. A diagram of the TC locations is shown in Figure 2.

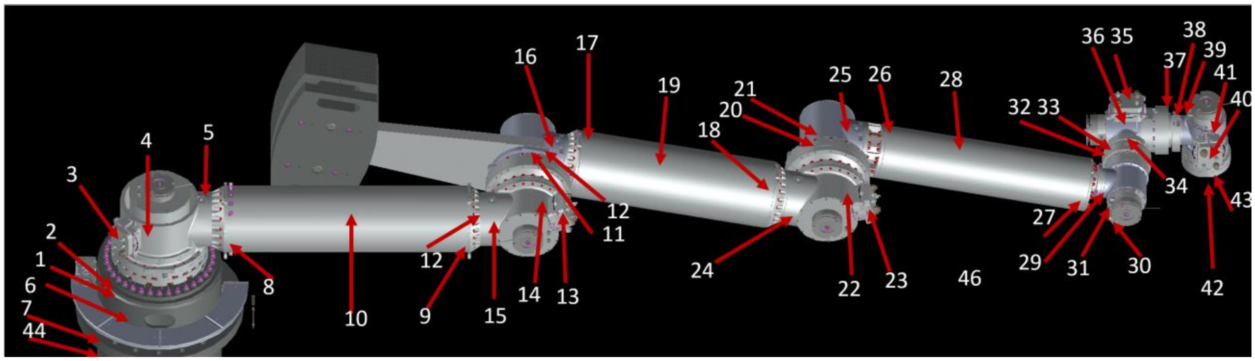

Figure 2. TC locations for the TVAC test.

TCs were used due to existing availability of equipment, despite the challenges of installing on a moving system. In order to not impede movement, the TCs were routed from the point of application back down the length of the arm to the base of the arm, with slack created at the joints. The power and control wiring for the arm was already bundled in this manner, so the TCs were attached to the existing wire bundle. The TC wiring was then routed to the chamber pass-through connections. A general layout of the wiring path is shown below.

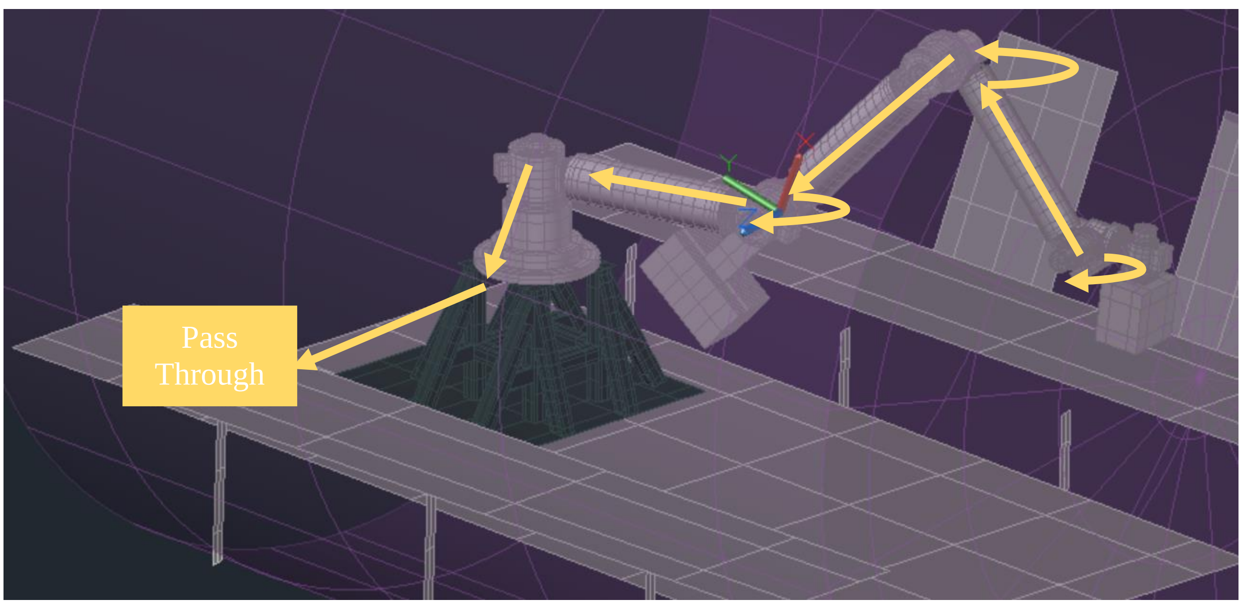

Figure 3. TC wiring follows the highlighted path.

All TCs were installed using Kapton tape to electrically isolate them from the arm, then covered with a layer of aluminum tape. A few inches of wire away from each TC bead, another piece of aluminum tape was applied to the TC wire to reduce the strain on the TC bead installation from the movement of the arm. An example of one TC with strain relief is shown in Figure 4. The motion of the arm was slow enough to be difficult to observe, so there would be little jostling of the TCs due to the arm's inertia. The most likely source of TC detachment would be the movement of the wiring leading back to the wiring pass-through point in the chamber, which is why the strain relief application was crucial. TCs were placed in locations on the points of interest that best aligned with the planned movement of the arm.

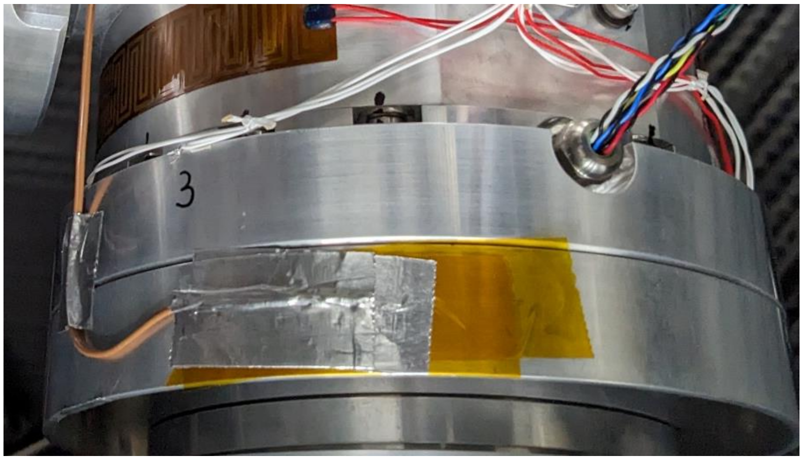

Figure 4. Close-up of one TC installation.

After installing the TCs and other sensors, the pre-test procedure required movement checks not in vacuum to ensure the arm was operational. An unintended consequence of adding the TC wiring down the length of the arm in the existing wiring bundles was that the bundles became much stiffer and therefore inhibited some of the test movements of the arm during these pre-test checks. This was particularly apparent at the wire bundles on the smaller joints, where the bundles were initially created with sufficient slack to allow rotation in all directions, but after the addition of the stiffer TC wire, did not move with the joints as easily. This issue was corrected by bundling the TC wires around the end joints separate from the larger bundle and with longer slack to allow the required movement.

Additionally, permanent TCs are installed throughout the shroud to record the shroud temperature. This provides information needed for modeling the thermal environment around the arm.

Test Procedure

The test procedure was broken into three iterations: initial vacuum movement, heated movement, and cold movement. Each iteration repeated the same motion commands sent to the arm, but with a different environment. The initial movement had neither intentional cooling or intentional heating while the movements were being completed. The electric strip heaters on the joints were then heated until the joints measured 57°C and the movements were repeated. After this set of movements, the heaters were set to maintain 0°C while the shroud was flooded with LN_2. Once the shroud fill was complete and the arm had cooled to the point the heaters turned on to keep it from getting below 0°C, the movements were repeated for a final time.

The motion commands were to move each joint individually through its allowable range of motion and then transition from a straight position as shown in Figure 2, where all the joints are at 0°, into a nominal operating position as shown in Figure 5. ICON defined a series of motions to simulate nominal operations slewing the arm and lowering the end of the arm near the floor.

Since the test was exploratory, several halts were called at varying times to troubleshoot hardware or software issues. An unintended benefit of this extended test was a portion of unallocated time on the schedule after the hot test was completed before cold operations could start due to shift schedule availability. The thermal team used this opportunity to try to achieve a thermal steady state in the time allowed. The heaters were set to maintain 35°C and all other power to the arm was turned off. The arm was allowed to come to a steady state of <= 0.01°C / hour rate of change, as measured by a subset of the 44 TCs.

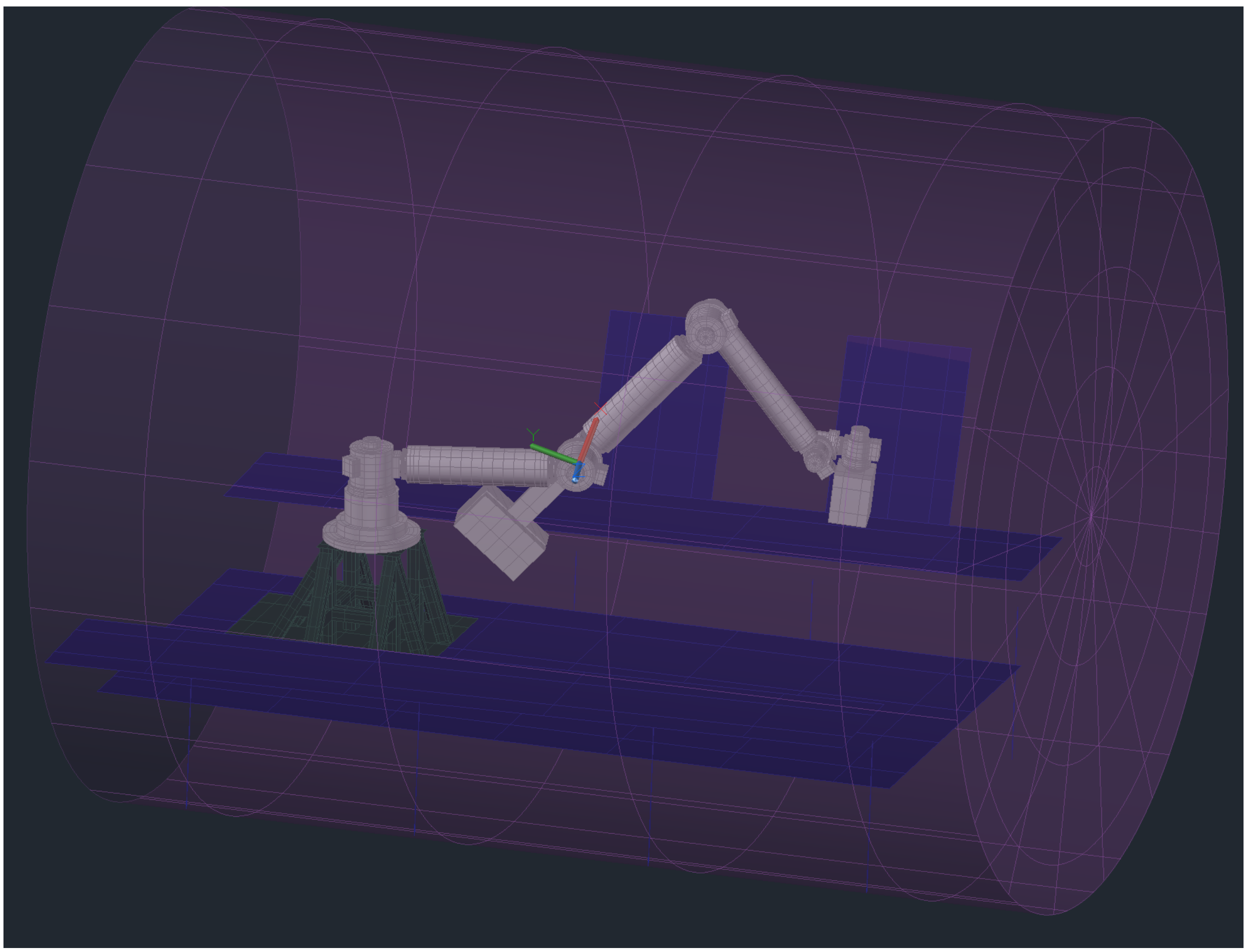

Figure 5. Nominal operating position shown inside V20 chamber model in TD.

The thermal steady state was achieved after six hours, with data from all 44 TCs recorded. This made it possible to correlate the previously uncorrelated thermal model to steady state data. ICON recorded the current draw to the heaters and provided the voltage ratings for the heaters, allowing for power calculations for the heat dissipation of the system.

TEST RESULTS

The TC installation was successful, as none of the TCs showed signs of detachment when examined after the TVAC test was complete.

The results showed the arm did reach the steady state parameters, with the temperature of the TCs varying between 16°C and 35°C. The full set of plotted TC data versus time for the steady state run is shown in Figure 6. The wave pattern seen in a few of the TC lines is due to the heaters turning on and off on the smaller joints, which are more sensitive to the temperature fluctuations.

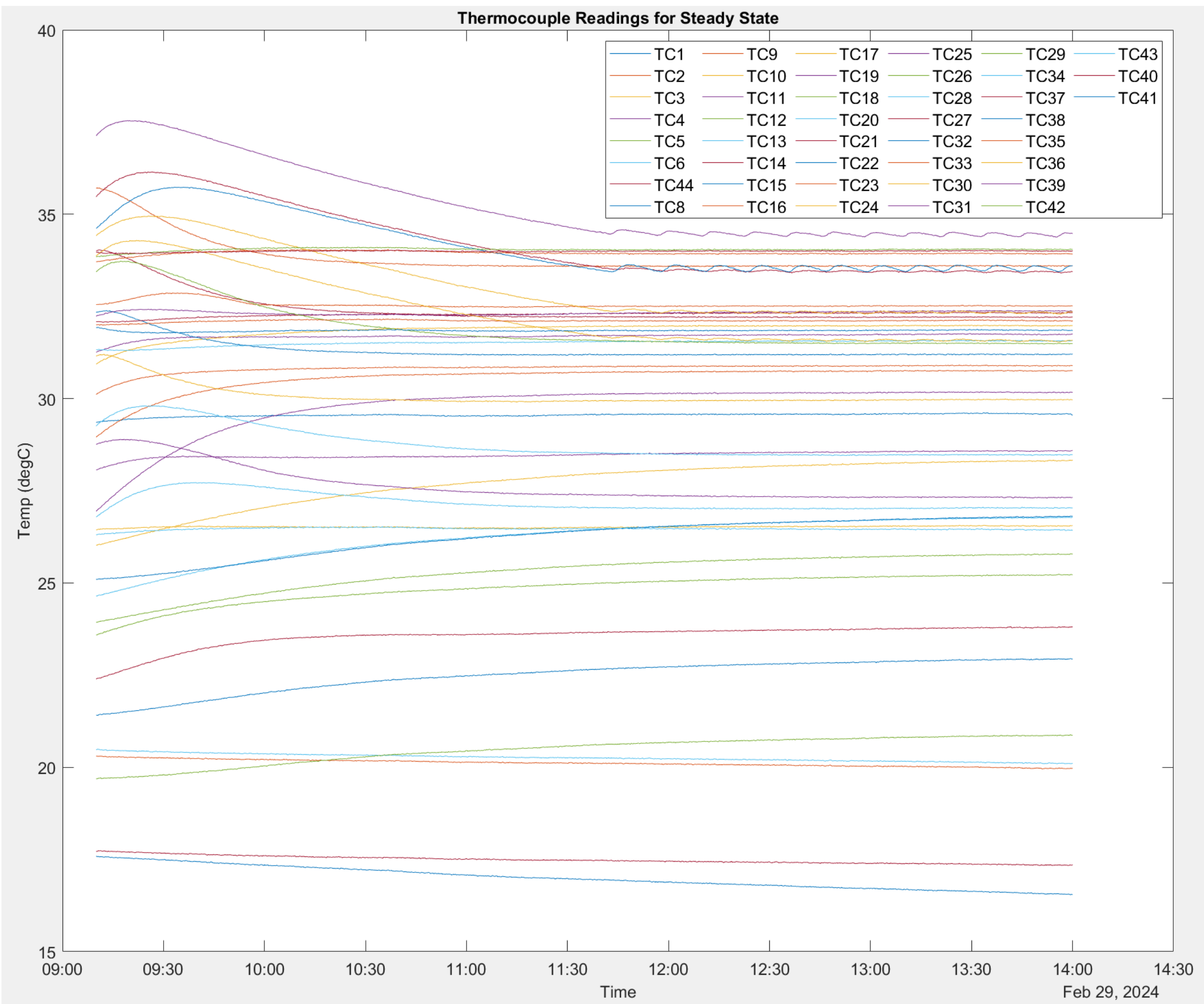

Figure 6. Thermocouple readings while the arm came to a thermal steady state.

THERMAL MODEL CORRELATION

The test results were used to correlate the thermal model. The thermal model was created in Thermal Desktop (TD), composed of TD primitive shapes based on the physical geometry of the terrestrial arm. The mounting pedestal was also created as TD primitive shapes. The radiative boundary conditions were defined by the V20 chamber, modeled as a TD primitive cylinder enclosing the arm and pedestal. The rolling cart surface, scavenger plates, and knee boards inside the chamber are also represented with TD primitive shapes and included in the radiation calculations. The thermal model is shown in Figure 5.

The heat input to the system was calculated from the recorded current data for each of the heaters multiplied by the known voltage, 24V, to determine the heater power in Watts. Nodes in the model were chosen to represent the placed TCs for comparison to the test data. The initial parameters for the model are shown in Table 3. The initial emissivity of the arm was based on the bare, unpolished aluminum surface. The G10 spacer interface contact coefficient was the thermal conductivity of G10. The joint thermal resistances refer to the resistance at the point of rotation. This is a sealed, lubricated ball bearing joint where the initial values for the thermal resistance were determined by TVAC testing at ICON's facility.

Table 3. Initial TD Model Parameters

Parameter	**Initial Value**
Emissivity (ε)	0.2
G10 spacer interface contact coefficient	0.014884 W/in^2/K
Large joint thermal resistance	0.524 K/W
Small joint thermal resistance	1.19 K/W

The initial model run with these values showed several discrepancies as compared to the test data. The first one investigated was the larger temperature gap across the G10 spacer in the model, which implied that there was a higher heat flux going across that spacer in the test than what was modeled. The spacer interface was initially assumed to have a uniform value of the thermal conductivity of G10. However, the pedestal attachment was so large and therefore required large bolts with 2" diameter. These bolts could provide a non-negligible path for heat transfer. The calculations to determine the net heat transfer across the G10 spacer and bolts are shown below. Using the bolt size, the heat flux was calculated using the properties of Aluminum 6061 and then the average heat transfer coefficient was calculated based on the fractional area of the G10 material and the bolts.

Constants

$$Abolt := \pi \cdot (1\ in)^2$$

$$lBolt := 0.5\ in$$

$$kAl := 4.5\ \frac{W}{in \cdot K}$$

$$G10g := 0.293\ \frac{W}{m \cdot K}$$

Thermal Conductivity (k*A/l)

$$boltQ := kAl \cdot \frac{Abolt}{lBolt} = 28.274\ \frac{W}{K} \qquad boltQ'' := \frac{kAl}{lBolt} = 9\ \frac{W}{in^2 \cdot K}$$

these are per bolt

$$G10Q := G10g \cdot \frac{268.138\ in^2}{0.5\ in} = 3.991\ \frac{W}{K} \qquad G10Q'' := \frac{G10g}{0.5\ in} = 0.015\ \frac{W}{in^2 \cdot K}$$

Proportional effect of bolts on surface

$$fraction := \frac{Abolt \cdot 20}{268.138\ in^2} = 0.234$$

this is the fraction of the total surface area the total bolt diameters take up

$$Gave := fraction \cdot boltQ'' + \frac{1}{fraction} \cdot G10Q'' = 2.172\ \frac{W}{in^2\ K}$$

Figure 7. Calculations for conduction through G10 spacer with aluminum bolts.

The difference between the TC value and the model value was plotted to determine if a temperature gradient existed based on location. Parametric cases were run to evaluate trade studies on the impact of the emissivity, ε, of the arm on the accuracy of the model. One trade study is shown in

Figure 8. The ε value was iterated between 0.15 and 0.25, with 0.175 (the orange line) best fitting the TC data. It is reasonable the ε was slightly lower than initially assumed, as the arm had cables and cable routing trays attached which would reduce the ability to radiate heat as compared to a bare metal surface.

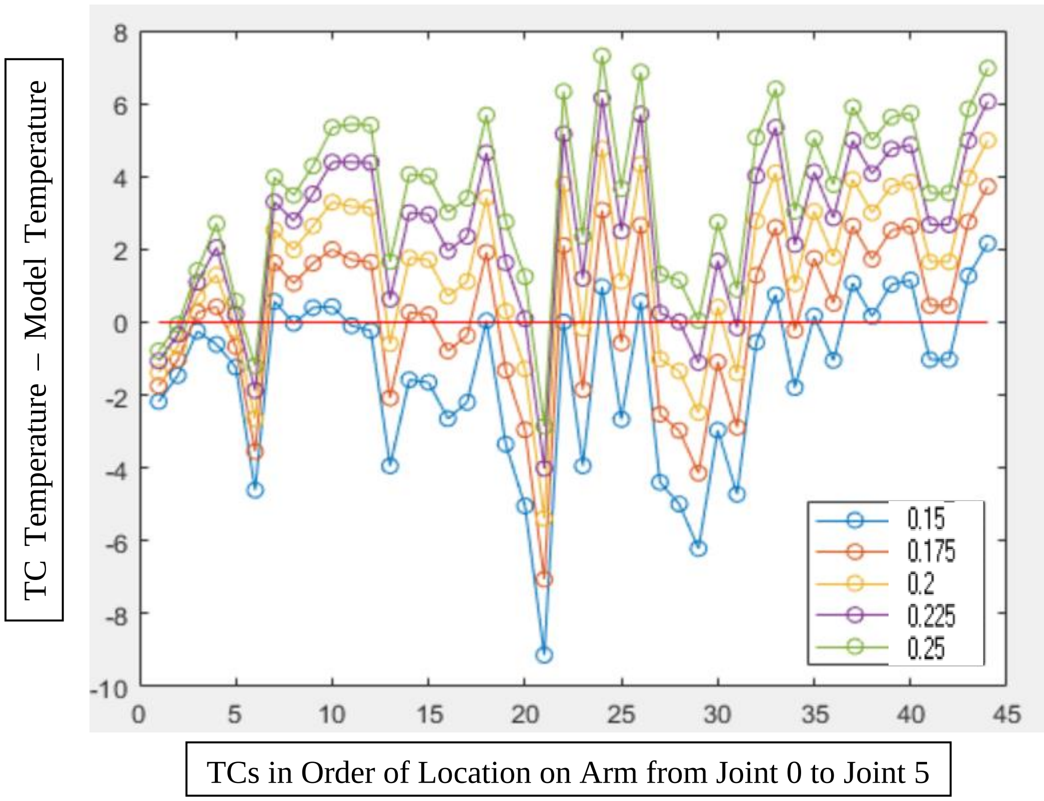

Figure 8. Emissivity trade study from ε = 0.15 to 0.25.

With the small joints (joints 3-5) consistently measuring warmer in the TC data than in the model, the ε for those joints was studied independently. These joints also had proportionally more of their surface area covered by cables due to their smaller size. The final trade study for the ε of the small joints is shown in Figure 9. 0.0625 was chosen as the best fit while still being conservative for the hot case.

With these ε values, the final temperature difference between the TCs and model are shown in Figure 10. All are within +/-5°C of the model data except for the highlighted TC. When the test data was examined, that particular TC (TC 18) was reading about 8°C colder than its neighboring TCs, so there could be an issue with how TC 18 was operating.

With these alterations correlating closely to the test data, no adjustments were needed for the thermal resistivity of the joints. These values were given by ICON before the V20 test and determined through TVAC testing of the joints at their facility.

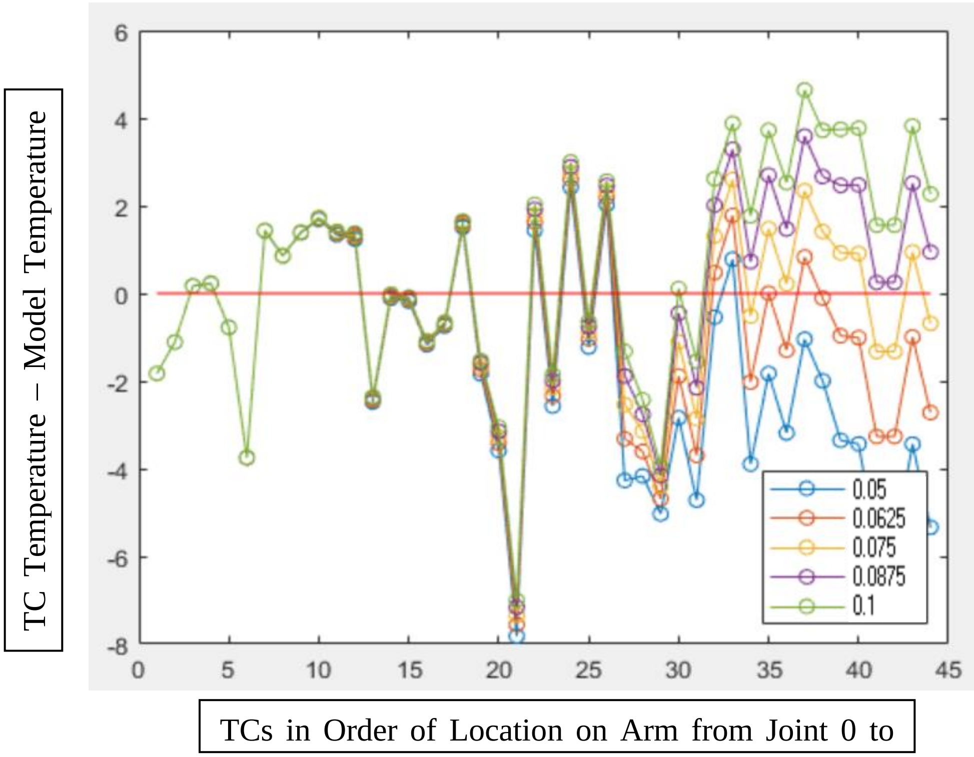

Figure 9. Emissivity trade study from ε = 0.05 to 0.1 for the arm between joints 3 and 5.

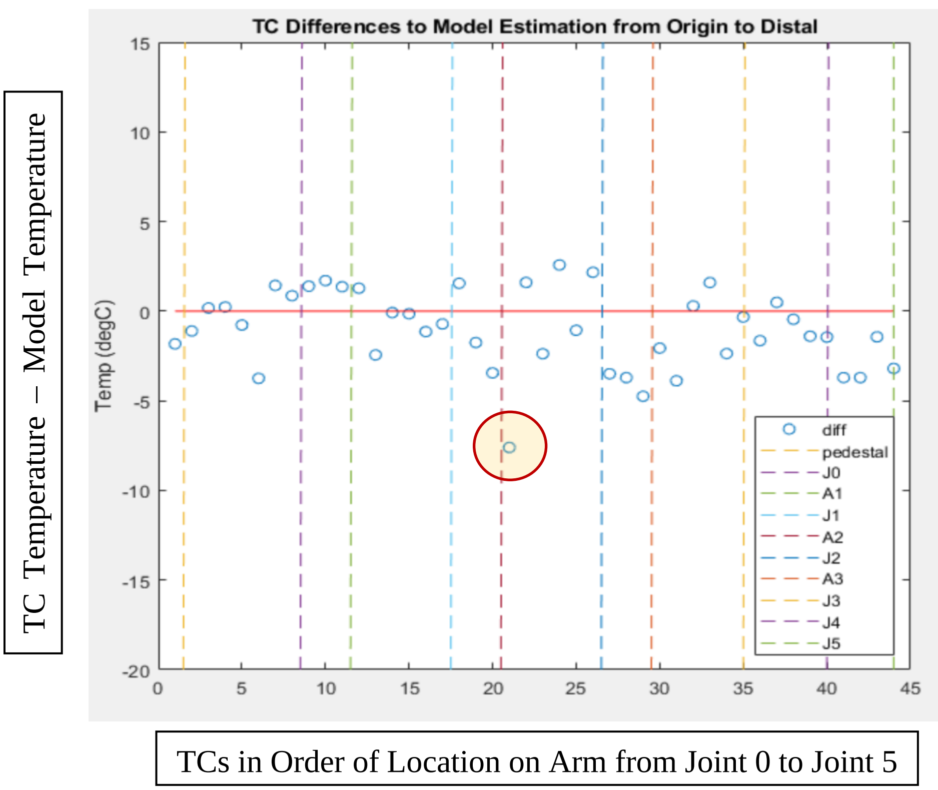

Figure 10. Final temperature delta between the test and model data.

The final model parameter values are shown in Table 4. The model values adjusted correlate to actual conditions during the test, with limited view factors to the arm and a higher path of thermal conductivity through the base of the arm.

Table 4. TD Model Parameters After Correlation

Parameter	**Initial Value**	**Final Value**
Emissivity (ε) of small joints (joints 3-5)	0.2	0.0625
Emissivity (ε) of the remainder of the arm	0.2	0.175
G10 spacer interface contact coefficient	0.014884 W/in^2/K	2.172 W/in^2/K
Large joint thermal resistance	0.524 K/W	0.524 K/W
Small joint thermal resistance	1.19 K/W	1.19 K/W

CONCLUSIONS

Gathering the thermal data was challenging, due to the size and motion of the arm. Routing the TC cables down the path of least interference and completing motion checkouts with the TCs attached before beginning the TVAC portion of the test was invaluable for successful data gathering. The additional Aluminum tape for strain relief also proved vital to keeping the TCs fully in contact with the arm and not moving due to tension on the cables as the arm moved.

The thermal steady state achieved was a reliable point of information to correlate the model. However, this correlation has limitations. There was only one steady state case to correlate to, which could mask inaccuracies that would be triangulated if there was another steady state or controlled input transient test to examine. The other temperature data gathered during the test generally has conditions too complicated to accurately replicate for an initial correlation, with motors and brakes firing for short durations and not settling to a constant temperature before operating again. If this test was conducted again in the future, additional thermal steady state testing with varying heater set points or with varying TVAC boundary temperatures would be beneficial to improve the accuracy of the thermal model.

ACKNOWLEDGEMENTS

This author would like to thank Stephanie Mauro (MSFC), Dan Popok (MSFC-ESSCA), and Parker Weide (MSFC) for their guidance and assistance.